UDK 577.083.3+579.84

POLYADHESINS: AN ARMORY OF GRAM-NEGATIVE PATHOGENS FOR PENETRATION THROUGH THE IMMUNE SHIELD

V. P. ZAV'YALOV

Joint Biotechnology Laboratory, Department of Chemistry,
University of Turku, Turku, Finland
Kherson State University, Kherson, Ukraine

E-mail: vlazav@utu. fi

Received 08.07.2013

The rapid emergence of treatment-resistant bacterial pathogens has become a major threat to public health. The outbreak of new Shiga-toxin–producing *Escherichia coli* O104H4 infection occured in Germany in 2011 illustrates this problem. To colonize host tissues, pathogenic bacteria express surface adhesive organelles. The German strain uses aggregative adherence fimbriae I (AAF/I) to anchor to the intestinal mucosa and induce inflammation. AAF/I belong to the family of chaperone/usher assembled fimbrial polyadhesins. Polyadhesins are functioning as an armory for penetration through the host immune shield. The polyadhesin-binding to the target cells triggers subversive signal by aggregation of host cell receptors that allow pathogens to mislead and evade immune defense. Their binding is orchestrated with the type III secretion system, which is extremally important for bacterial virulency. Polyadhesins also are involved in biofilm formation making bacteria more resistant to immune response. Because of this, the polyadhesins are potential targets for immune countermeasures against bacterial infections, in particular for anti-adhesion therapy with antibodies to polyadhesins as one of alternatives to antibiotic therapy.

Key words: Gram-negative pathogens; polyadhesins; anti-immune armory.

Adhesive organelles of bacterial pathogens are crucial virulence factors, mediating attachment to the target cells of their hosts and initiating infectious process. They also are involved in biofilm formation making bacteria more resistant to immune response.

Gram-negative pathogens possess two major classes of proteinaceous adhesins [1]:

- The fimbrial adhesive organelles, represented by the linear homopolymers or heteropolymers (up to 7 distinct subunits) of hundreds to thousands of protein subunits;
- The non-fimbrial adhesins consisted of a single protein or homotrimers.

The superfamily of fimbrial organelles, assembled by the chaperone/usher (CU) machinery, is divided in two functionally distinct families: monoadhesins and polyadhesins [1, 2].

Monoadhesins comprises in main the thick rigid and thin flexible adhesive pili of a complex subunit composition (up to 7 distinct subunits), which typically display only one adhesive domain on the tip of the pilus. The assembly of monoadhesins is assisted with the FGS (having a short F1-G1 loop) class of periplasmic chaperones [3, 4]. The monoadhesins are encoded in main by the gene clusters of the γ1-, γ2-, γ4-, and γ-monophyletic groups [5].

Polyadhesins, typically, have non-pilus, amorphous or capsule-like morphology. They either comprise homopolymers, which consist of only one type of subunit, or heteropolymers, which consist up to 6 distinct subunits. The notable property of polyadhesins is that all subunits of homopolymers or one of the main structural subunits of heteropolymers possesses one or two independent binding sites specific to different host cell receptors [1, 2]. Assembly of one subfamily of polyadhesins is assisted with the FGL (having a long F1-G1 loop) class of periplasmic chaperones [3, 4]. FGL chaperone-assembled polyadhesins are encoded exclusively by the gene cluster of the

γ3-monophyletic group [5]. The assembly of another subfamily of polyadhesins is assisted with the FGS class of chaperones. FGS chaperone-assembled polyadhesins are encoded in main by the gene cluster of the κ-monophyletic group [5]. Recently a novel member of polyadhesin family, the *Escherichia coli* common pilus (ECP), has been revealed [6]. The ECP has the unique architecture. It is composed of two sequentially combined polyadhesive homopolymers of EcpA and EcpD subunits, recpectively, with a dual role in biofilm formation and host cell recognition. The ECP is assembled via alternative CU pathway [7] and encoded by the gene cluster related to the α-monophyletic group [5].

Polyadhesins are functioning as an armory for penetration through the host immune shield. The polyadhesin-binding to the target cells triggers subversive signal by aggregation of host cell receptors that allow pathogens to mislead and evade immune defense [1, 2]. Their binding is orchestrated with the type III secretion system, which is extremally important for bacterial virulency [8]. Polyadhesins also are involved in biofilm formation making bacteria more resistant to immune response [6]. Because of this, the polyadhesive organelles are potential targets for immune countermeasures against bacterial infections, in particular for anti-adhesion therapy with antibodies as one of alternatives to antibiotic therapy [9, 10].

Several excellent reviews focused on the results of the structure/functional studies of FGS-chaperone assembled fimbrial monoadhesins have been published recently. Among the later were the reviews by [11–15]. However, the last comprehensive review on the structure, function, phylogenesis and clinical applications of polyadhesins was published by us more than three years ago [1]. The recently accumulated significant knowledge on different aspects of biogenesis of the growing family of Gram-negative polyadhesins and their clinical applications requires a new analysis and generalization.

ORGANIZATION OG GENE CLUSTERS ENCODING POLYADHESINS

Genes of proteins involved in the expression and assembly of polyadhesive fibers via the CU pathway are arranged into compact gene clusters, which are located either on the chromosome or on the plasmids of Gram-negative bacteria. Depending on the structural properties of periplasmic chaperones and phylogenetic classification, suggested by [5], they can be divided into three families:

- FGL chaperone-comprising gene clusters related to the γ3-monophyletic group;
- FGS chaperone-comprising gene clusters related to the κ-monophyletic group;
- Alternative chaperone-comprising gene cluster(s) related to the α-monophyletic group.

FGL Chaperone-Comprising Gene Clusters related to the γ3-Monophyletic Group

Our studies, which opened the way to finding a family of polyadhesins, began with the cloning and sequencing of the genes responsible for the formation of the capsule of *Yersinia pestis*, the causative agent of pneumonic plague.

Encoded by the *caf* gene cluster fraction 1 (F1), capsular antigen from *Y. pestis* comprises aggregated high-molecular-weight linear polymers of a single subunit Caf1 [1, 2, 8, 16-18]. The genes of the *caf* gene cluster, *caf1*, *caf1M*, *caf1A* and *caf1R*, encode, respectively, for Caf1 subunit, periplasmic chaperone Caf1M, an outer membrane assembler, the molecular usher Caf1A and the protein Caf1R regulating gene cluster transcription [19–32].

The *psa* gene cluster from *Y. pestis* encodes proteins for expression and assembly of the fimbrial pH6 (Psa) antigen comprising the high-molecular-weight polymer of the PsaA subunit [33]. PsaB functions as the periplasmic chaperone and PsaC as the molecular usher. Two additional proteins, PsaE and PsaF, have been shown to regulate the transcription of the *psaA* gene [34]. Another transcriptional regulator, RovA, interacts with the *psaE* and *psaA* promoter regions, suggesting that RovA is an upstream regulator of the *psa* gene cluster [35]. Identical *psa* gene clusters are present in *Y. pestis* and *Y. pseudotuberculosis* [33].

Closely related to the *psa* gene cluster of *Y. pestis*, *Y. enterocolitica* contains *myf* encoding the Myf fimbriae, which are built up of MyfA subunits [36]. The *psa* and *myf* clusters have a similar general organization. Moreover, proteins encoded by these gene clusters display a significant sequence similarity, suggesting that the pH6 (Psa) antigen and Myf fimbriae have a common function in the different species of *Yersinia*. Like PsaE and PsaF encoded by *psa*, the MyfE and MyfF proteins encoded by *myf* play a role in the regulation of cluster transcription [37].

The *cs-3* gene cluster from *E. coli* encodes for proteins for expression and assembly of the

colonization factor-3 that forms CS-3 fimbriae comprising the high-molecular-weight polymer of the CS-3 subunit [38]. CS3-E functions as the periplasmic chaperone and CS3-D as the molecular usher.

The *nfa* gene cluster from *E. coli* encodes proteins for the expression and assembly of the nonfimbrial adhesin, NFA-I, comprising the high-molecular-weight polymer of the NfaA subunit [39]. NfaE functions as the periplasmic chaperone and NfaE as the molecular usher.

A group of *E. coli* gene clusters, *afa-3*, *afa-8*, *agg*, *aaf*, *agg-3*, *dafa*, *dra* and *daa*, which encode proteins for the expression and assembly of the afimbrial adhesins Afa-III and AfaE-VIII, the aggregative adherence fimbria type I, II and III (AAF/I, AAF/II and AAF-III), the diffuse adherence fibrillar adhesin (Dafa), the Dr hemagglutinin flexible fimbriae and the F1845 (DaaE) fimbrial adhesin, respectively, have a peculiar feature: each gene cluster encodes additional subunit D, for which an invasive function was suggested (putative invasin subunit) [40, 41]. DraE and AfaE-III adhesins may assemble into a flexible fiber, which provides the link between the usher at the outer membrane and the putative invasion subunit located at the tip of the fiber [42–44]. However, expression of DraD invasin subunit is independent of the DraC usher and DraE fimbrial subunit [45]. In addition, polymerization of DraE fimbrial subunits into fimbrial structures does not require the expression of DraD. Then, it was shown that type II secretion in *E. coli* strain Dr1 leads to DraD translocation to the bacterial cell surfaces [46]. Later, it was demonstrated that the DraD subunit is not required for β1 integrin recruitment or bacterial internalization [47, 48]. Therefore, the function of D subunits is still in question.

The *Salmonella* spp. gene clusters *saf*, *sef*, *cs6-1* and *cs6-2*, which encode proteins for the expression and assembly of the atypical fimbriae Saf, the filamentous fimbriae-like structures SEF14/18 and the colonization factors CS6-1 and -2, respectively, have another common peculiar feature: all of these gene clusters encode two adhesin subunits. The SefB chaperone of *S. enteritidis* assists in the assembly of two distinct cell-surface structures, SEF14 and SEF18, which are homopolymers of SefA and SefD subunits, respectively [49]. The CssC chaperone assists in assembling thin CS6 fibrillae, which are composed of two heterologous CssA and CssB subunits [50].

FGS Chaperone-Comprising Gene Clusters related to the κ-Monophyletic Group

The gene cluster *pef* is responsible for expression of plasmid encoded (PE) fimbriae of *S. typhimurium* composed of only one structural subunit, which probably functions as an adhesin subunit. A cosmid carrying the *pef* operon was introduced into *E. coli* and expression of fimbrial filaments composed of PefA was confirmed by flow cytometry and immune electron microscopy [51]. PE fimbriae were purified from the surface of *E. coli* and the resulting preparation was shown to contain PefA as the sole major protein component. Binding of purified PE fimbriae to a glycan array suggested that this adhesin specifically binds the trisaccharide Galss1–4 (Fuca1–3) GlcNAc, also known as the Lewis X (Lex) blood group antigen.

The gene clusters *fan*, *lda*, *fae* and *ral* encode proteins for the expression and assembly of the F4 (K88), Lda and F5 (K99) thin flexible pili and rabbit-specific enteropathogenic *E. coli* (REPEC) fimbriae of *E. coli*, respectively [52–54]. These pili/fimbriae consist of four or five subunits. However, F4 (K88), F5 (K99) and Lda pili do not display specialized adhesive domains on the tip of the pilus, but carry binding sites on their main structural subunit (FanG, FaeG and LdaG) [52, 54, 55]. The overall arrangement of the *ral* gene cluster closely resembles that of the *fae* cluster, with homologous genes occupying the same relative position in each cluster. The *ral* cluster also has some of the more specific features of the *fae* cluster, such as the overlapping reading frames of the genes encoded chaperone and usher and the apparent absence of promoters within the region carrying the structural genes [53]. This general similarity, together with the significant levels of homology exhibited by individual genes, makes it reasonable to propose functions for the *ral* gene products based on the known roles of their Fae counterparts. Thus, it was proposed that RalC, RalF and RalH are minor fimbrial subunits of the fimbrial structure, which is primarily composed of RalG, the major fimbrial subunit [53]. The gene cluster *afr* encodes proteins for the expression and assembly of the *E. coli* AF/R1 pili [56]. The subunits encoded by the *afr* gene cluster have the highest percentage amino acid identity with the subunits encoded by the *ral* cluster [53].

The *fed* gene cluster, encoding the F18 fimbriae, is composed of five genes, encoding the major subunit FedA, the usher protein FedB, the periplasmic chaperone FedC, the minor

pilin FedE and the adhesin FedF [57, 58]. Based on usher phylogeny, the *fed* cluster falls into the κ-fimbrial clade of CU systems [5]. However, it was demonstrated [59] that FedF, the F18 adhesin responsible for ABH glycosphingolipid binding, is a two domain adhesin typical for monoadhesive fimbrial organelles.

Alternative Chaperone-Comprising Gene Cluster(s) related to the α-Monophyletic Group

The most characterized member of this new family, *ecp* (or *mat*) gene cluster, encodes the *E. coli* common pilus (ECP), composed of two sequentially combined polyadhesive homopolymers of EcpA and EcpD subunits, respectively, with a dual role in biofilm formation and host cell recognition [6]. The *ecp* operon is composed of six genes: *ecpR, ecpA, ecpB, ecpC, ecpD*, and *ecpE*. Examination of EcpR revealed its function as transcriptional regulator [60], whereas primary sequence analysis of EcpB, EcpC, and EcpE [6] detected low but significant similarity with a variety of chaperone and usher proteins from the CU family [5]. The typical sequence identity is <17% with all known usher (EcpC) and chaperone (EcpB and EcpE) structures. Although sequence analysis of EcpD (~60 kDa) revealed no matches with other proteins, inspection of the N termini in EcpA and EcpD showed a significant level of similarity [6]. The *mat* (or *ecp*) gene cluster was related to the α-monophyletic group of alternative CU pathway [5, 7].

The ECP is highly conserved between enteric bacterial species [6]. *Serratia proteamaculans*, *S. odorifera*, *Klebsiella sp.*, *K. pneumoniae*, and *Enterobacter cancerogenus* possess fimbrial subunits with high homology to EcpA (80%, 82%, 98%, 97%, and 96% sequence identity, respectively), which may suggest a role for ECP in stabilizing multispecies biofilms by interactions through EcpA orthologs.

STRUCTURE OF POLYADHESIN SUBUNITS

Structure of Chaperone-Complemented Subunits

Chaperone-free subunits of fimbrial polyadhesins [18, 24] and monoadhesive fimbriae/pili [61, 62] are highly unstable and prone to form aggregates. Hence, structural information on many subunits of these organelles was obtained by studying chaperone–subunit complexes [17, 18, 63–67].

Figure 1 shows ribbon diagrams of the Caf1M–Caf1 [17, 18] and SafB–SafA [66] complexes. These complexes reveal the chaperone-bound conformation of FGL chaperone-assembled polyadhesin subunits. The polyadhesin subunits Caf1 and SafA have an incomplete immunoglobulin-like fold. Despite the lack of significant sequence similarity, polyadhesin subunits display similar organization of the B, C, E and F β-strands, which are known to form a common structural core of the immunoglobulin-like fold [68]. End of the F1–G1 loop and the beginning of the G1 β-strand in Caf1M harbor a subunit-binding motif of five alternating bulky hydrophobic residues (V126, V128, V130, F132 and I134) [17, 18]. The same region in the SafB molecule harbors a similar five-residue motif of one small hydrophobic (A114) and four bulky hydrophobic residues (L116, L118, L120 and I122) [66]. The rest of the F1–G1 loop (residues 104–123 in Caf1M and 104–113 in SafB) is disordered in the crystal structures. Another subunit-binding motif in FGL chaperones of three alternating hydrophobic residues (Y12 in Caf1M/F12 in SafB, V14 and I16) is localized in a long N-terminal sequence, which forms the A1 strand. A1 and G1 β-strands are the edge strands of the β-sandwich fold of the N-terminal domain. In the complex A1 and G1, β-strands are extended due to the partial

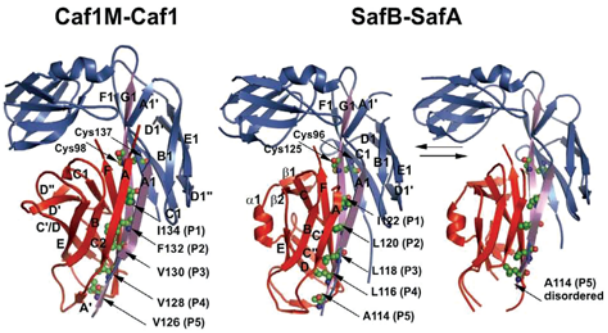

Fig. 1. **Ribbon presentation of the crystal structures of Caf1M–Caf1 and SafB–SafA complexes.** The chaperones are blue with G1 and A1 edge strands in violet; the subunits are red. The two conserved Cys residues in the whole FGL family that form disulfide bond are shown as ball-and-stick. The hydrophobic residues in the G1 strand of the chaperones that interact with the P5–P1 pockets of the subunits are also shown as ball-and-stick. The SafB residue A114, which interacts with the P5 pocket, is in equilibrium between a bound (left, type I structure) and an unbound (right, type II structure) state in the P5 pocket. The structures were redrawn based on the coordinates of atoms published by [17, 18] (PDB accession number 1P5V) and [66] (PDB accession numbers 2CO6 and 2CO7). All figures were prepared with PYMOL [69]

ordering of the N-terminal sequence and the F1–G1 loop, respectively, to form a binding platform, exposing the hydrophobic residues of the binding motifs. In addition to this binding structure, Caf1M and SafB chaperones apply a pair of conserved positively charged residues (R20 and K139 in Caf1M and R20 and K127 in SafB) to bind subunits by anchoring their C-terminal carboxyl groups.

Fig. 2, *A, C* illustrate how the Caf1 subunit is complemented by the Caf1M chaperone [17, 18]. The absence of the seventh (G) strand results in a six-stranded β-sandwich where the hydrophobic core of Caf1 is partially exposed in a long and deep hydrophobic groove. Caf1 interacts mainly with the N-terminal domain in Caf1M (Fig. 1). These two proteins bind via edge strands in Caf1 and in the N-terminal domain of Caf1M to form a closed barrel with a common core [17]. Strand G1 in Caf1M is hydrogen-bonded to strand F in Caf1. Chaperone A1 strand is hydrogen-bonded to subunit strand A. Hydrophobic residues from the Caf1M chaperone G1 strand are donated to the Caf1 subunit to compensate for the missing G strand (Fig. 1 and 2). The longer G1 donor strand of the Caf1M chaperone inserts a motif of five bulky hydrophobic residues (P1–P5 residues; Fig. 1 and 2) into five binding pockets in the hydrophobic groove of the Caf1 subunit (P1–P5 binding pockets).

The crystal structures of the Caf1M–Caf1 and SafB–SafA complexes show a considerably larger interactive area between the chaperone and the subunit than that found in the FGS chaperone–pilin complexes [63–65, 67]. This is a result of the presence of a more extended hydrophobic groove in the Caf1 and SafA subunits than in pilus subunits, which is complemented by subunit-binding motifs of Caf1M and SafB containing the additional FGL-specific sequences. However, the major F1–G1–loop–G1 β-strand-binding motif of SafB contains four rather than five bulky hydrophobic residues (L116, L118, L120 and I122), which interact with the hydrophobic P4–P1 pockets of the subunit's groove. The fifth donor residue inserting into pocket P5 is a small A114. Two crystal forms of the SafB–SafA complex were observed that differ in the extent of ordering around A114 (Fig. 1) [66]. In type I crystals, A114 is ordered and is inserted into the P5 pocket of the SafA subunit (Fig. 1). In type II crystals, this residue is disordered and does not insert into the P5 pocket (Fig. 1). As a result, the loops and secondary structure elements in the SafA subunit that form this P5 pocket are also disordered

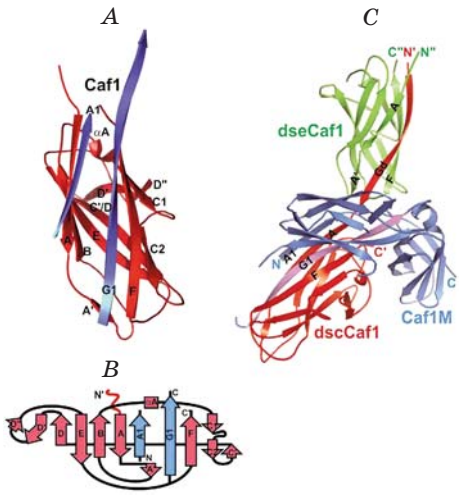

Fig. 2. **Structure of the Caf1 polyadhesin subunit complemented with Caf1M chaperone (*A*, *C*).** The Caf1 polyadhesin subunit is shown in red with donor strands from Caf1M chaperone (blue). Only interacting chaperone–subunit strands are shown. *B* — Ribbon diagram of the native Caf1M–Caf1′–Caf1″ complex. Caf1M is blue, except for G1 and A1 β-strands (violet). The chaperone-bound Caf1′ subunit and N-terminal donor strand (Gd) are red; the Caf1″ subunit corresponding to the tip of growing fiber is green. The N- and C-termini are labeled in the same colours as the ribbons. The redrawing is based on the coordinates of atoms of structures published by [17, 18] (PDB accession numbers 1P5V and 1Z9S). *A* and *C* were prepared with PYMOL [69]

and are not observed in the electron density map. These two structures suggest equilibrium between the two states of the SafB–SafA complex as a result of a weak binding of the chaperone G1 donor strand at the P5 site of the SafA-binding groove [66].

Structure of Subunits in the Fiber

The elucidation of crystal structure of *Y. pestis* F1 minimal fiber Caf1M–Caf1′–Caf1″ (ternary complex) was an important step in understanding the general principles of subunit assembly via the CU pathway. This structure revealed the fiber conformation of the organelle subunit (Caf1″) and subunit–subunit interactions in fibers [17, 18]. The structure of Caf1M and the chaperone-bound Caf1′ subunit is virtually the same as in the Caf1M–Caf1 binary preassembling complex. However, in contrast to the disordered N-terminal region of Caf1 in binary complex, the N-terminal region of Caf1′ is ordered and forms an antiparallel donor β-strand interaction with the last (F) β-strand of the chaperone-free Caf1″ subunit (Fig. 2, *B*). The donated strand produces a bona fide immunoglobulin-like

topology in the fiber subunit. The N-terminal donor strand was denoted as 'Gd' (d for donor) because it plays the same structural role in the fiber as it does in the (C-terminal) G strand of the canonical immunoglobulin fold [17]. Thus, the release of the subunit from the chaperone–subunit complex and its incorporation into a growing fiber involves an exchange of G1 and A1 donor strands of the chaperone to the Gd strand of the neighboring subunit in the fiber. The replacement of the G1 strand by the Gd strand also involves a change of direction of the donor strand from parallel to antiparallel to the F β-strand of the subunit. This process was predicted earlier for FGS chaperone-assembled adhesive pili [63, 64] and for FGL chaperone-assembled polyadhesins [16] and was termed 'donor-strand exchange'. A similar 'topological transition' [65] was also observed for the P pilus subunit PapE bound to a peptide designed to have the sequence of the proposed donor strand of the PapK subunit, suggesting that the donor-strand exchange takes place during assembly of both types of the organelles.

Chaperones preserve Folding Energy of Subunits for Driving of the Fiber Assembly

No energy input from external sources is required to convert periplasmic chaperone–subunit preassembly complexes to free chaperone and secreted fibers [70], in spite of a much more extensive interface between a chaperone and a subunit than that between fiber subunits [17]. Some clues as to how the process can be energetically driven have been provided by structural studies [17, 18, 65, 67]. Comparison of a chaperone complemented (Caf1′) with a fiber subunit (Caf1″) revealed a large conformational difference [17, 18]. The fiber conformation was referred to as the 'closed' or the 'condensed' conformation [18]. The observed difference between open and closed conformations, involving a rearrangement and condensation of the subunit hydrophobic core, suggested that periplasmic chaperones might trap subunits in a high-energy molten globule-like folding intermediate state [17]. A model was proposed in which release of the subunit, followed by Gd donor-strand complementation, allows folding to be completed, driving fiber formation [17]. In contrast to the bulky hydrophobic donor residues in the chaperone G1 donor strand, many smaller donor residues in the subunit N-terminal Gd donor segment do not intercalate between the two sheets of the subunit β-sandwich, allowing close contact between the two sheets [17, 18].

A significant stabilizing contribution from the final fine packing of the hydrophobic core of the subunit is suggested by the melting of the native ternary complex. Structurally observed complete collapse of the Gd-complemented fiber Caf1″ subunit results in a dramatic increase in enthalpy and transition temperature for melting the fiber module. Thermodynamic studies provide strong evidence for the hypothesis that collapse of the subunit hydrophobic core shifts the equilibrium toward fiber formation [18].

Recently, the mutagenesis of the binding motifs of the Caf1M chaperone and Caf1 capsular subunit was performed and analyzed the effect of the mutations on the structure, stability, and kinetics of Caf1M–Caf1 and Caf1–Caf1 interactions [32]. The results suggest that a large hydrophobic effect combined with extensive main-chain hydrogen bonding enables Caf1M to rapidly bind an early folding intermediate of Caf1 and direct its partial folding. The switch from the Caf1M–Caf1 contact to the less hydrophobic, but considerably tighter and less dynamic Caf1–Caf1 contact occurs via the zip-out–zip-in donor strand exchange pathway with pocket 5 acting as the initiation site.

MOLECULAR ARCHITECTURE OF ADHESINS

The final architecture and morphology of linear fibers depend on the subunit composition and the mode of subunit–subunit interactions. These factors determine a coiling of secreted linear fibers into different structures. Fig. 3, *A* shows the scheme of coiling of FGS chaperone-assembled thick rigid monoadhesive pili with a diameter of 7–8 nm. The data on the architecture of monoadhesins were reviewed by [11–15, 71–76]. The scheme of FGS chaperone-assembled thin flexible heteropolyadhesins with a diameter of 2–4 nm is shown in Fig. 3, *B*. The data on the architecture of FGS chaperone-assembled heteropolyadhesins were reviewed by [77]. The scheme of FGS chaperone-assembled homopolyadhesins with a diameter of about 2 nm is shown in Fig. 3, *C* [51]. The structures of FGL chaperone-assembled polyadhesins with a diameter of about 2 nm are shown in the Fig. 3, *D* and *E* [42, 78]. Fig. 3, *F* and *G* show the structures of alternative chaperone-assembled polyadhesin ECP [6], composed of two sequentially combined polyadhesive homopolymers of EcpA and EcpD subunits, respectively (Fig. 3, *F*), with a dual role in biofilm formation

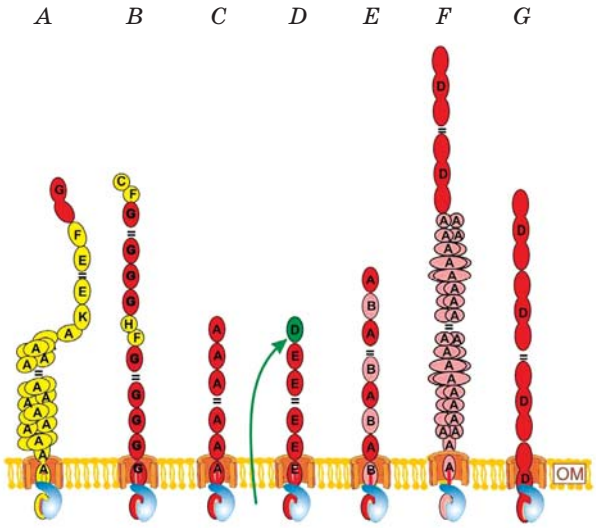

Fig. 3. ***A* — Schematic presentation (elaborated by the authors) of the structure of FGS chaperone-assembled thick rigid monoadhesive fimbriae/pili (P pili as example) [75, 76]; *B* — FGS chaperone-assembled hetero-polyadhesins (F4, K88 pili as example) [77]; *C* — FGS chaperone-assembled homo-polyadhesins (PE fimbriae as example) [51]; *D, E* — FGL chaperone-assembled polyadhesins (*D* — AfaE polyadhesin as example [42]; *E* — CS6 heteropolyadhesin as example [78]); *F, G* — alternative chaperone-assembled polyadhesin ECP [6] composed of two sequentially combined polyadhesive homopolymers of EcpA and EcpD subunits, respectively (*F*), with a dual role in biofilm formation and host cell recognition or polyadhesive homopolymer of EcpD subunits (*G*) with a separate role in host cell recognition.**

Periplasmic chaperones and outer membrane ushers are in blue and light orange, respectively. Adhesin subunits are in red. Structural subunits are in yellow. Green arrow shows chaperone/usher-independent secretion of AfaD subunit (shown in green) via type II secretion system [46] and its potential display on the tip of the AfaE fimbrial polyadhesin [42]

and host cell recognition and polyadhesive homopolymer of EcpD subunits (Fig. 3, *G*) with a separate role in host cell recognition. The scanning electron microscopy images show that the pili of EcpA subunits are thin flexible fibers that extend several micrometers away from the bacterial surface and have a high tendency to aggregate into well-ordered parallel and 12-nm antiparallel superstructures, implicating an important role for EcpA in biofilm formation [6]. The FGL chaperone-assembled polyadhesins can aggregate to form amorphous masses or capsules, for example the F1 capsular antigen [79], NFA-I [39], NFA-I-like Dr-II [80] or afimbrial adhesins III, VII and VIII [40, 81].

In the case of FGS chaperone-assembled monoadhesive fimbriae/pili, the specialized adhesive subunit always occurs at the tip of fimbriae, either as the distal end of thin (~2.5 nm) and flexible fimbriae (e.g. F17G from F17 fimbriae) or at the edge of a thin (~2.5 nm) tip fibrillum that is stuck onto a relatively rigid, 1–2-mm-long and ~7.5-nm-wide right-handed helical pilus rod (e.g. PapG of P pili and FimH of type I pili) (Fig. 3, *A*) [82]. This specialized subunit is called an adhesin. All adhesive subunits of monoadhesive fimbriae/pili are two-domain adhesins [63, 82–86]. A two-domain adhesion consists of an N-terminal receptor-binding domain that can be stably expressed on its own and a rather conserved C-terminal pilin domain. Both domains have an immunoglobulin-like fold and are joined via a short interdomain linker. The few known crystal structures of tip-located receptor-binding N-terminal adhesin domains of monoadhesive fimbriae/pili, PapGII, FimH and F17G/GafD, show that, despite little or no sequence identity, common to them all is an elongated β-barrel jelly-roll fold that contains the receptor-binding groove [63, 82–86]. The adhesin domains differ in disulfide patterns, the size and location of the ligand-binding groove, as well as in the mechanism of receptor binding. In particular, their glycan-binding sites have evolved in different locations onto this similar scaffold, and with distinct, highly specific binding properties.

Subunits of monoadhesive fimbriae are called pilins. In particular, P fimbriae are composed of ~1000 copies of the major subunit protein PapA, which polymerize to form a rigid stalk connected to a flexible tip consisting of limited copies of the minor subunit proteins PapE and PapF and receptor-binding adhesin PapG at the distal end [87, 88]. Type I pili are composed of up to 3000 copies of the subunit FimA, which form a stiff, helical pilus rod, and subunits FimF, FimG and FimH, which form the linear tip fibrillum. All subunits in the pilus interact via the donor-strand complementation, in which the incomplete immunoglobulin-like fold of each subunit is complemented by insertion of an N-terminal extension from the following subunit.

In the case of FGL chaperone-assembled polyadhesins, all subunits may possess two independent binding sites specific to different host-cell receptors [42, 43, 46, 47, 89–91]. Dimensions of the bacterial polyadhesive fibers Dr, whose assembly is assisted by the FGL chaperone, were investigated with negative-stain electron microscopy [42]. Thin flexible fibers (2 nm diameter) were observed. The results are entirely consistent with the model with end-to-end contact between each subunit (Fig. 5) [42] and are reminiscent of the model

of capsular F1 antigen from *Y. pestis*, Caf1 [17]. Similar thin fibers have been observed for the pH6 antigen [33]. In addition to the predominance of thin fibers Dr, the electron microscopy also revealed a thicker morphology with overall dimensions larger than the linear model suggested [42]. Thick fibers are not consistent with end-to-end contact and imply that more extensive intersubunit interactions also exist. This would rigidify the resulting rod by the tighter coiling of a single fiber or formation of a trimeric coiled-coil arrangement of fibers.

The ultrastructure of the *Y. pestis* capsule was examined with whole bacteria and negative stain transmission electron microscopy [92]. Bacteria were grown to the logarithmic phase at 37 °C, pH 7.4. The appearance of the capsule was more clearly visible than reported in previous studies, in which the capsule generally appeared as an amorphous haze or as a dense mass surrounding the bacteria [79, 93, 94]. The *Y. pestis* KIM61 strain consistently produced an extended halo composed of thin fibrils and denser aggregates. This denser capsular material, likely composed of aggregates of the thin fibrils, sometimes extended out from the bacterial surface in long strands. The thin, fibrillar appearance of the F1 capsule resembles structures previously reported for other members of the FGL family of chaperone/usher pathways, including the pH6 antigen of *Yersinia* [33, 36] and the CS3 and CS6 pili of ETEC [95, 96]. The negative-stain electron microscopy and single-particle image analysis was used to determine the 3D structure of the *S. typhimurium* Saf polyadhesin [97]. The Saf polyadhesin comprises highly flexible linear multisubunit fibers that are formed by globular subunits connected to each other by short links, giving a 'beads on a string'-like appearance. Quantitative fitting of the atomic structure of the SafA polyadhesin subunit into the electron density maps, in combination with linker modeling and energy minimization, has enabled analysis of subunit arrangement and intersubunit interactions in the Saf polyadhesin. Short intersubunit linker regions provide themeans for flexibility of the Saf polyadhesin by acting as molecular hinges that allow a large range of movement between consecutive subunits in the fiber.

FUCTIONS OF POLYADHESINS

Common Features of Anti-Immune and Proinflammatory Activities of Polyadhesins

In contrast to mono-adhesive pili, which possess only one binding domain on the tip of the pilus (Fig. 4, *A*), each poly-adhesive fiber potentially might (Fig. 4, *B*) [1, 2, 8]:

- ensure a powerful polyvalent fastening of a bacterial pathogen to a host target cell;
- aggregate host-cell receptors and trigger transduction of signals, causing immunosuppressive and proinflammatory responses;
- pull a bacterium to a host cell by a zipper-like mechanism that increases tightness of the contact.

A tight contact between interacting cells hampers diffusion of Ca^{2+} in the site of contact and consequently triggers the Ca^{2+}-dependent type III secretion system (encoded by the pCD1 virulence plasmid) that destroys the defense activity of the host cell [98–101]. This is extremely important for bacterial virulence. In particular, *Y. pestis* appears to utilize the type III secretion pathway to destroy cells with

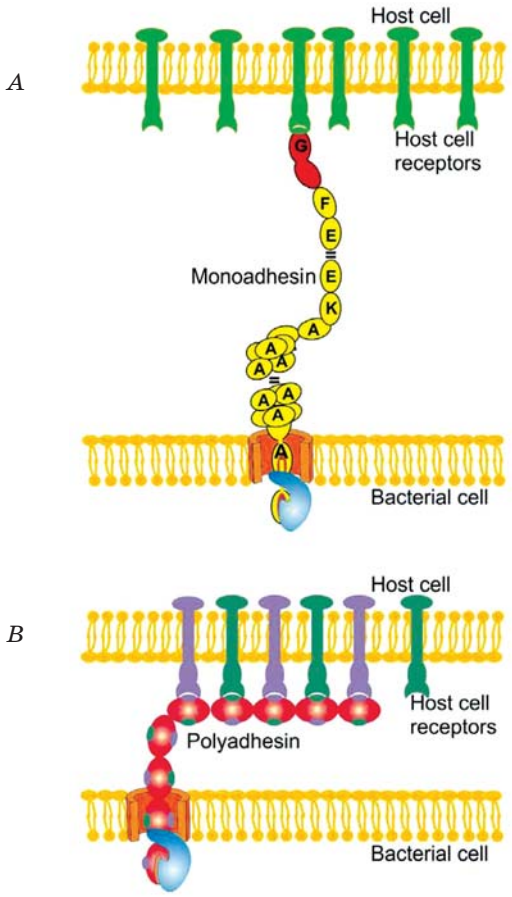

Fig. 4. **Schematic illustration (elaborated by the author) of a binding of monoadhesins (*A*) and polyadhesins (*B*) to host-cell receptors.**
Periplasmic chaperones and outer membrane ushers are in blue and orange, respectively. Adhesin and pilin subunits are in red and yellow, respectively. Host receptors for monoadhesins are shown in green. Two different types of host receptors for polyadhesins are shown by violet and greencyan

innate immune functions (macrophages, dendritic cells and neutrophils), which represent the first line of defence thereby preventing adaptive responses and precipitating the fatal outcome of plague [102]. It was found that dendritic cells infected with *Y. pestis* failed to adhere to solid surfaces and to migrate toward the chemokine CCL19 in an *in vitro* transmembrane assay. Both effects were dependent on the presence of a pCD1 plasmid, and on bacterial growth shift to 37 °C, before infection [103].

It was found that *Y. pestis* adhesins facilitate Yop delivery to eukaryotic cells and contribute to plague virulence [104]. The Ail, plasminogen activator (Pla) and pH6 antigen (Psa) could mediate Yop translocation to host cells. The contribution of each adhesin to binding and Yop delivery was dependent upon the growth conditions. When compared to an *ail* mutant, additional deletion of *psaA* (encoding Psa) led to a 130,000-fold increase in LD_{50} in mice relative to the KIM5 parental strain. These results indicate that Psa can serve as environmentally-specific adhesin to facilitate Yop secretion, a critical virulence function of *Y. pestis*.

Binding of Polyadhesins to Host-Cell Receptors

Afa/Dr polyadhesins — Afa/Dr polyadhesins Dr, F1845 (DaaE), NFA-I and AfaE-III adhesins allow binding to the Dra blood-group antigen presented on the CD55/decay-accelerating factor (DAF), a complement-regulatory and signaling molecule [105]. Under physiological conditions, CD55/DAF plays a central role in preventing the amplification of the complement cascade on host-cell surfaces [106, 107]. CD55/DAF interacts directly with membrane-bound C3b or C4b and prevents the subsequent uptake of C2 and factor B.

The residues of AfaE-III adhesion involved in CD55/DAF binding were localized (Fig. 5) [42]. The binding regions for AfaE-III and the complement pathway convertases lie in close proximity to each other on CD55/DAF. Binding of adhesin Dr to CD55/DAF is inhibited by chloramphenicol, whereas binding of AfaE-III is unaffected [105, 108]. This was used to locate the DraE adhesive site. The 3D structure of the strand-swapped trimer of wild-type DraE in complex with chloramphenicol was solved. NMR data supported the binding position of chloramphenicol within the crystal [43, 44]. Chloramphenicol binds to a surface pocket between the N-terminal portion of strand B and the C-terminal portion of strand E and lies within the recently identified CD55/DAF-binding site (Fig. 5) [42].

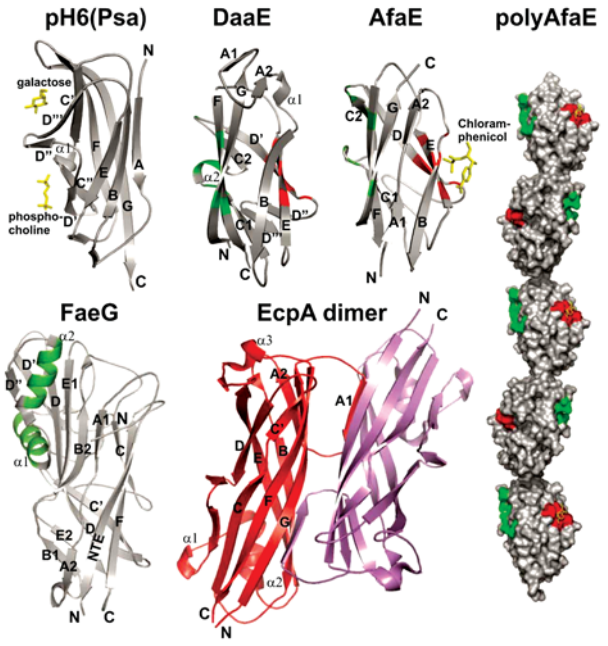

Fig. 5. **Binding sites of FGL chaperone-assembled polyadhesin subunits DaaE and AfaE, FGS chaperone-assembled polyadhesin subunit FaeG and alternative chaperone-assembled polyadhesin subunit EcpA.**

Ribbon diagrams presentations of the DaaE subunit of a strand-swapped trimer of wild-type DaaE of F1845 adhesin and a self-complemented AfaE subunit of AFA-III adhesin with chloramphenicol as a yellow stick presentation. CD55/DAF- and CEACAMS-binding sites derived from DraE and DaaE mutagenesis are shown in green and red, respectively. Molecular surface rendering of a model for the AfaE fiber was generated by assuming the same orientation between successive subunits as observed for Caf1′ and Caf1″ in the F1 fiber [17]. The residues involved in binding with CD55/DAF and CEACAMS are in green and red, respectively. The binding site in FaeG is shown by green. The redrawing is based on the data and coordinates of atoms of the structures published by [6, 42–44, 55, 89, 90, 117]. The figures were prepared with PYMOL [69]

The 3D structure of DaaE at resolution 1.48E also was solved [90]. Trimers of the protein were found in the crystal, as has been the case for other adhesins Dr. Naturally occurring variants and directed mutations in DaaE have been generated and analyzed for their ability to bind CD55/DAF. Mapping of the mutation sites onto the DaaE molecular structure shows that several of them contribute to a contiguous surface that is likely the primary CD55/DAF-binding site (Fig. 5).

Dr, F1845 (DaaE) and AfaE-III adhesins also interact with carcinoembryonic antigen (CEA)-related cellular adhesion molecules CEACAM1, CEACAM5 and CEACAM6 [109]. This recognition is followed by activation of

CEACAMS-associated signaling by pathogens triggering the cellular events. CEACAM1, CEACAM5 and CEACAM6 belong to the immunoglobulin superfamily of adhesion molecules [110]. CEACAM1 has been shown to be expressed in leukocytes, including granulocytes, activated T cells, B cells and natural killer cells [111]. CEACAM1 acts as a novel class of immunoreceptor tyrosine-based inhibition motif-bearing regulatory molecules on T cells that are active during the early phases of the immune response in mice [112–116].

Random mutagenesis with functional analysis and chemical shift mapping by NMR show a clear-cut CEACAMS binding site located primarily in the A, B, E and D strands of the adhesin Dr subunit (Fig. 5) [89]. This site is located opposite the β-sheet encompassing the previously determined binding site for CD55/DAF, which implies that the polyadhesin Dr can bind simultaneously to both receptors on the epithelial cell surface. The structure of the CEA/Dr adhesin complex was proposed based on NMR spectroscopy and mutagenesis data in combination with biochemical characterization [47, 91]. The Dr adhesin/CEA interface overlaps appreciably with the region responsible for CEA dimerization. Binding kinetics, mutational analysis and spectroscopic examination of CEA dimers suggest that adhesins Dr can dissociate CEA dimers before the binding of monomeric forms [47, 91].

pH 6 (Psa) polyadhesin — It was found by flow cytometry that individual *Y. pestis* cells can express the capsular F1 antigen concomitant with the pH6 antigen (Psa) on their surface when analyzed [94]. Isogenic Δ*caf* (F1 genes), Δ*psa* and Δ*caf*Δ*psa* mutants were constructed and studied with the three respiratory tract epithelial cells. The Δ*psa* mutant bound significantly less to all three epithelial cells compared with the parental wild-type strain and the Δ*caf* and Δ*caf*Δ*psa* mutants, indicating that the pH6 antigen acts as an adhesin for respiratory tract epithelial cells.

It was found that the pH6 antigen of *Y. pestis* is a novel bacterial immunoglobulin G (IgG)-binding receptor [118]. A pseudoimmune complex with human IgG1, IgG2 and IgG3 was formed. No binding to human IgG4, rabbit, mouse or sheep IgG was found. Antigen pH6 binds the human IgG1 Fc subunit and does not bind Fab and pFc' subunits. This finding may be explained by pH6 antigen binding to the β1-linked galactosyl residue [119] in a carbohydrate moiety of human IgG1, IgG2 and IgG3 that is linked to CH_2 domains of their Fc subunit [120].

Purified pH6 antigen selectively binds to apolipoprotein B-containing lipoproteins (low-density lipoproteins) in human plasma [121].

Binding of purified recombinant pH6 antigen to gangliotetraosylceramide, gangliotriaosylceramide and lactosylceramide was indicated by an enzyme-linked immunosorbent assay (ELISA) [119].

It was found that pH6 (Psa) antigen fimbriae mediate bacterial binding to human alveolar epithelial cells [122]. The receptor of the pH6 antigen was identified as phosphatidylcholine. The results indicate that the pH6 antigen uses the phosphorylcholine moiety of phosphatidylcholine as a receptor to mediate bacterial binding to pulmonary surfactant and alveolar epithelial cells [122].

The crystal structure of PsaA in complex with both galactose and phosphocholine reveals separate receptor binding sites that share a common structural motif, thus suggesting a potential interaction between the two sites (Fig. 5) [123]. Mutagenesis of this shared structural motif identified Tyr126, which is part of the choline-binding consensus sequence but is found in direct contact with the galactose in the structure of PsaA, important for both receptor binding. Thus, this structure depicts a fimbrial subunit that forms a polymeric adhesin with a unique arrangement of dual receptor binding sites.

F4 (K88) polyadhesin — Enterotoxigenic *E. coli* expressing F4 (K88) fimbriae are the major cause of porcine colibacillosis and are responsible for significant death and morbidity in neonatal and postweaned piglets. F4 fimbriae are assembled into thin, flexible polymers mainly composed of the single-domain adhesin FaeG [55, 77, 117]. FaeG has an Ig core made up of strands A1, A2, B1, B2, C, D, E1, E2, F and G, named according to their place in the Ig-fold and in analogy to the nomenclature used for other fimbrial subunit structures (Fig. 5) [55, 117]. These show an incomplete Ig-like structure, lacking the last β-strand G. In pili, this G-strand is provided by the Nte of the adjacent subunit. In the Ig fold of the FaeG, a short helical turn occurs between strands A2 and B1, and an extra strand C′ is inserted between strands C and D. In addition to the Ig-folded core, the FaeG structure contains an extra domain introduced between strands D and E1. This domain is composed of strands D′ and D″, linked by two α-helices, α1 and α2.

The receptor binding site on FaeG was described as a spatial arrangement of two amino acid residues with a hydrophobic side-chain

(Phe/Leu134 and Phe/Leu/Met147) in combination with one or more amino acid residues with hydrophilic and charged side-chains (Lys/Arg136, Arg/Ser/His155 and Asp/Asn216, or in the hypervariable region comprised of residues 163–173) [52]. The structure of FaeG allowed to localize the aforementioned residues and the hypervariable regions comprising residues 163–173 and residues 206–216 on the surface of FaeG (Fig. 5, shown by green) [117]. This suggests that the receptor-binding site of FaeG is not located within the Ig core of the protein but rather in the extra domain made up of strands D′ and D″, and α-helices α1 and α2. Especially the long loop between D′ and α1 and the loop connecting the extra domain to the Ig core (between D″ and E1) are indicated as being part of the binding site.

ECP (Mat) polyadhesin — First data on a novel fimbria isolated at low temperatures from *E. coli* associated with newborn meningitis and septicaemia (NMEC) were published by [124]. This surface organelle was called the meningitis associated and temperature regulated (Mat) fimbria, although later by other groups was shown that this fibrillar organelle is ubiquitous across most *E. coli* strains and it is now usually referred to as the *E. coli* common pilus (ECP) [125–128]. *E. coli* are primarily commensal colonizers of the human and other animal bowels and they contribute to a healthy immune system of the host. There are also a number of virulent strains that can cause diarrheal diseases such as hemorrhagic colitis [129]. Furthermore, if they enter extraintestinal sites these strains can also lead to neonatal meningitis, urinary tract infections, sepsis, and pneumonia [130].

ECP fibres are assembled via the alternative CU pathway and the organelles are formed from polymerization of two pilin subunits (Fig. 3, *F* and *G*) [6]. The tip of ECP is uniquely composed from a polymerized array of a novel adhesive subunit EcpD (~ 60 kDa) recognizing an unknown ligand on the host cell surface [6]. The majority of ECP is composed of an 18 kDa domain called EcpA [124, 125], which functions in binding hydrophobic surfaces and mediating interbacterial aggregation in early biofilm formation [6, 131].

The crystal structure of EcpA from uropathogenic *E. coli* has been recently solved (Fig. 5; PDB: 3QS2, 3QS3) [6]. Like other CU major pilin domains, EcpA is formed from an incomplete Ig-like fold, where an adjacent molecule in the fiber donates its N-terminal strand (N-terminal extension) to fill a hydrophobic groove running along the full length of EcpA, completing the very stable Ig-like motif (Fig. 5). EcpA is fashioned from approximately 50% hydrophobic residues and the surface is scattered with hydrophobic patches including a number of aromatic residues. This likely promotes a less-specific contact with a wide range of hydrophobic substrates and polymers.

ECP are quite flexible with a width ~6 nm, which consistently varies along the fibre length (Fig. 3, *F*) [6]. Electron microscopy images of *E. coli* producing ECP show these fibres form a mesh that encapsulates the whole microcolony. ECP interacts with itself through pili crossing over one another, parallel fibre entwining and antiparallel entwining [6]. The crystal lattice of EcpA also revealed an intertwining of antiparallel fibres giving rise to a super helical diameter of ~12 nm. EcpA is highly conserved amongst a range of other enteric bacterial species including *Serratia proteamaculans*, *Serratia odorifera*, *Klebsiella sp.*, *Klebsiella pneumoniae*, and *Enterobacter cancerogenus*, which suggests a role for ECP in establishing contacts between multiple species [6].

CONCLUSIONS AND FUTURE PERSPECTIVES

Among the bacterial causes, enterotoxigenic *E. coli* (ETEC), *E. coli* strains producing enterotoxins, are the most common cause of diarrheal disease in children living in endemic areas, as well as children and adults traveling to these areas. Approximately 280–400 million ETEC-associated diarrhea cases occur annually in children younger than 5 years old, plus 100 million more cases in children older than 5 years, which results in approximately 300,000–500,000 deaths annually [132]. Travelers are also susceptible to diarrhea as they are usually immunologically naive and are exposed to the environment in developing countries. Among the causes of traveler's diarrhea, ETEC is the most common. It was estimated that 400 million adult diarrheal cases are associated with ETEC [132].

After half a century of highly productive antibiotic development, however, it has now become obvious that antibiotics cannot provide the ultimate solution in the fight against bacterial infections. The non-critical use of antibiotics in human and veterinary medicine has caused widespread resistance in bacteria. Antibiotic-resistant strains of Gram-negative pathogens have emerged extensively in the

last dozen years, whereas safe and effective vaccines against many of them are currently not available. There are now a growing number of reports of cases of infections caused by Gram-negative organisms for which no adequate therapeutic options exist [133, 134]. This return to the preantibiotic era has become a reality in Europe as well as in other parts of the world. A large outbreak of diarrhea and the hemolytic-uremic syndrome caused by an unusual serotype of Shiga-toxin-producing *E. coli* (O104:H4) occured in Germany in 2011. A large number of cases of diarrhea caused by Shiga-toxin-producing *E. coli* (STEC) have been reported — 3167 without the hemolytic-uremic syndrome (16 deaths) and 908 with the hemolytic-uremic syndrome (34 deaths) — indicating that this strain is notably more virulent than most of the STEC strains [135]. The pAA plasmid of C277-11 (referred to here as pAA C277-11) encodes the *agg* cluster responsible for expression of the aggregative adherence fimbriae Type I, AAF-I. The AAF-I fimbriae are related to the family of polyadhesins [17]. The main subunit of the AAF-I fimbriae, AggA, together with the additional subunit AggB may be used for development of vaccine against this STEC strain. Among the most common protective antigens for design of vaccines against ETEC are the CS3 and CS6 polyadhesins [132].

Passive immunization has recently become an even more attractive approach because of individuals with impaired immune systems who are unable to respond to conventional vaccines. Also, passively administered antibodies have the ability to provide rapid and immediate protection. Anti-bacterial serum therapy is now being reinvented in modern biotechnology terms, in the form of monoclonal antibodies [10]. However, when considering antibody production for passive immunotherapy applications for treatment of enteric bacterial infections, chickens present a much more economical source of large quantities of specific antibodies [9]. Chiken IgY yields have been reported to range from 60 to 150 mg IgY per egg. Given that a typical hen can lay approximately 325 eggs per year, this can result in a potential yield of around 20–40 g of IgY per year, of which 2% to 10% is antigen-specific [9].

IgY has been tested against a number of enteric pathogens. IgY produced against the porcine ETEC polyadhesins F4 (K88) and F5 (K99) was found to inhibit the binding of *E. coli* K88-, K99-positive strains to porcine epithelial cells and porcine intestinal mucus *in vitro* [9]. When given orally to piglets, these antibodies dose-dependently protected against *E. coli* infection. It was found that when anti-$K88^+$ ETEC IgY was encapsulated in chitosan-alginate microparticles, it exerted its anti-diarrheal effects much faster (24 h versus 72 h postinfection in pigs given nonencapsulated IgY) and led to increased weight gain when compared to pigs fed nonencapsulated antibodies [9]. The passive protective effect of anti–*E. coli* IgY in cattle has also been shown. Neonatal calves fed milk containing anti-ETEC IgY had transient diarrhea, 100% survival, and improved body weight gain [9].

Thus, the polyadhesins are potential targets for immune countermeasures against bacterial infections, in particular for anti-adhesion therapy with antibodies to polyadhesins as one of alternatives to antibiotic therapy.

This work was supported by grants from the European Commission/ Research Executive Agency under a Marie Curie International Incoming Fellowship (235538) and a grant from the Academy of Finland (112900).

REFERENCES

1. *Zav'yalov V., Zavialov A., Zav'yalova G., Korpela T.* Adhesive organelles of Gram negative pathogens assembled with the classical chaperone/usher machinery: structure and function from a clinical standpoint // FEMS Microbiol. Rev. — 2010. — V. 34, N 3. — P. 317–378.
2. *Zavialov A., Zav'yalova G., Korpela T., Zav'yalov V.* FGL chaperone-assembled fimbrial polyadhesins: anti-immune armament of Gram-negative bacterial pathogens // Ibid. — 2007. — V. 31, N 4. — P. 478–514.
3. *Zav'yalov V., Zav'yalova G., Denesyuk A., Korpela T.* Modelling of steric structure of a periplasmic molecular chaperone Caf1M of *Yersinia pestis*, a prototype member of a subfamily with characteristic structural and functional features // FEMS Immunol. Med. Microbiol. — 1995. — V. 11, N 1. — P. 19–24.
4. *Hung D., Knight S., Woods R. et al.* Molecular basis of two subfamilies of immunoglobulin-like chaperones // EMBO J. — 1996. — V. 15, N 15. — P. 3792–3805.
5. *Nuccio S., Bðumler A.* Evolution of the chaperone/usher assembly pathway: fimbrial classification goes greek // Microbiol. Mol. Biol. Rev. — 2007. — V. 71, N 4. — P. 551–575.
6. *Garnett J., Martнnez-Santos V., Saldaca Z. et al.* Structural insights into the biogenesis and biofilm formation by the *Escherichia coli* com-

mon pilus // Proc. Natl. Acad. Sci. USA. — 2012. — V. 109, N 10. — P. 3950–3955.
7. *Korea C., Ghigo J., Beloin C.* The sweet connection: Solving the riddle of multiple sugar-binding fimbrial adhesins in *Escherichia coli*: Multiple *E. coli* fimbriae form a versatile arsenal of sugar-binding lectins potentially involved in surface-colonisation and tissue tropism // Bioessays. — 2011. — V. 33, N 4. — P. 300–311.
8. *Zav'yalov V.* Fimbrial polyadhesins: anti-immune armament of *Yersinia* // Adv. Exp. Med. Biol. — 2012. — V. 954. — P. 183–201.
9. *Kovacs-Nolan J., Mine Y.* Egg yolk antibodies for passive immunity // Annu. Rev. Food Sci. Technol. — 2012. — V. 3. — P. 163–182.
10. *Oleksiewicz M., Nagy G., Nagy E.* Anti-bacterial monoclonal antibodies: Back to the future? // Arch. Biochem. Biophys. — 2012. — V. 526, N 2. — P. 124–131.
11. *Allen W., Phan G., Waksman G.* Pilus biogenesis at the outer membrane of Gram-negative bacterial pathogens // Curr. Opin. Struct. Biol. — 2012. — V. 22, N 4. — P. 1–7.
12. *Busch A., Waksman G.* Chaperone-usher pathways: diversity and pilus assembly mechanism // Phil. Trans. R. Soc. B. — 2012. — V. 367, N 1592. — P. 1112–1122.
13. *Geibel S., Waksman G.* Crystallography and electron microscopy of chaperone/usher pilus systems // Adv. Exp. Med. Biol. — 2011. — V. 715. — P. 159–174.
14. *Kline K., Dodson K., Caparon M., Hultgren S.* A tale of two pili: assembly and function of pili in bacteria // Trends Microbiol. — 2010. — V. 18, N 5. — P. 224–232.
15. *Lo A., Moonens K., Remaut H.* Chemical attenuation of pilus function and assembly in Gram-negative bacteria // Curr. Opin. Microbiol. — 2013. — V. 16, N 1. — P. 85–92.
16. *Zavialov A., Kersley J., Korpela T. et al.* Donor strand complementation mechanismin the biogenesis of non-pilus systems // Mol. Microbiol. — 2002. — V. 45, N 4. — P. 983–995.
17. *Zavialov A., Berglund J., Pudney A. et al.* Structure and biogenesis of the capsular F1 antigen from *Yersinia pestis*: preserved folding energy drives fiber formation // Cell. — 2003. — V. 113, N 5. — P. 587–596.
18. *Zavialov A., Tischenko V., Fooks L. et al.* Resolving the energy paradox of chaperone-mediated fibre assembly // Biochem. J. — 2005. — V. 389, N 3. — P. 685–694.
19. *Galyov E., Smirnov O., Karlyshev A. et al.* Nucleotide sequence of the *Yersinia pestis* gene encoding F1 antigen and the primary structure of the protein // FEBS Lett. — 1990. — V. 277, N 1–2. — P. 230–232.
20. *Galyov E., Karlyshev A., Chernovskaya T. et al.* Expression of the envelope antigen F1 of *Yersinia pestis* is mediated by the product of *caf1M* gene having homology with the chaperone PapD of *Escherichia coli* // Ibid. — 1991. — V. 286, N 1–2. — P. 79–82.
21. *Karlyshev A., Galyov E., Smirnov O. et al.* A new gene of the *f1* operon of *Y. pestis* involved in the capsule biogenesis // FEBS Lett. — 1992. — V. 297, N 1–2. — P. 77–80.
22. *Karlyshev A., Galyov E., Abramov V., Zav'yalov V. caf1R* gene and its role in the regulation of capsule formation of *Y. pestis* // FEBS Lett. — 1992. — V. 305, N 1. — P. 37–40.
23. *Karlyshev A., Galyov E., Smirnov O. et al.* Structure and regulation of a gene cluster involved in capsule formation of *Y pestis* // Biological Membranes: Structure, Biogenesis and Dynamic, NATO-ASI Serias (Op den Kamp JAF, ed) Springer-Verlag, NewYork, NY. — 1994. — V. H-82. — P. 321–330.
24. *Zav'yalov V., Chernovskaya T., Chapman D. et al.* Influence of the conserved disulphide bond exposed to the putative binding pocket, on the structure and function of the immunoglobulin-like periplasmic molecular chaperone, Caf1M, of *Yersinia pestis* // Biochem. J. — 1997. — V. 324, N 2. — P. 571–578.
25. *Chapman D., Zavialov A., Chernovskaya T. et al.* Structure and functional significance of the FGL sequence of the periplasmic chaperone, Caf1M, of *Yersinia pestis* // J. Bacteriol. — 1999. — V. 181, N 8. — P. 2422–2429.
26. *Zavialov A., Batchikova N., Korpela T. et al.* Secretion of recombinant proteins via the chaperone/usher pathway in *Escherichia coli* // Appl. Environ. Microb. — 2001. — V. 67, N 4. — P. 1805–1814.
27. *MacIntyre S., Zyrianova I., Chernovskaya T. et al.* An extended hydrophobic interactive surface of *Yersinia pestis* Caf1M chaperone is essential for subunit binding and F1 capsule assembly // Mol. Microbiol. — 2001. — V. 39, N 1. — P. 12–25.
28. *Zavialov A., Knight S.* A novel self-capping mechanism controls aggregation of periplasmic chaperone Caf1M // Ibid. — 2007. — V. 64, N 1. — P. 153-164.
29. *Yu X., Visweswaran G., Duck Z. et al.* Caf1A usher possesses a Caf1 subunit-like domain that is crucial for Caf1 fibre secretion // Biochem. J. — 2007. — V. 418, N 3. — P. 541–551.
30. *Dubnovitsky A., Duck Z., Kersley J. et al.* Conserved hydrophobic clusters on the surface of the Caf1A usher C-terminal domain are important for F1 antigen assembly // J. Mol. Biol. — 2010. — V. 403, N 2. — P. 243–259.
31. *Yu X., Dubnovitsky A., Pudney A. et al.* Allosteric mechanism controls traffic in the chaperone/usher pathway // Structure. — 2012. — V. 20, N 11. — P. 1861–1871.
32. *Yu X., Fooks L., Moslehi-Mohebi E. et al.* Large is fast, small is tight: determinants of speed and affinity in subunit capture by a

periplasmic chaperone // J. Mol. Biol. — 2012. — V. 417, N 4. — P. 294–308.
33. *Lindler L., Tall B. Yersinia pestis* pH6 antigen forms fimbriae and is induced by intracellular association with macrophages // Mol. Microbiol. — 1993. — V. 8, N 2. — P. 311–324.
34. *Yang Y., Isberg R.* Transcriptional regulation of the *Yersinia pseudotuberculosis* pH6 antigen adhesin by two envelope-associated components // Ibid. — 1997. — V. 24, N 3. — P. 499–510.
35. *Cathelyn J., Crosby S., Lathem W. et al.* RovA, a global regulator of *Yersinia pestis*, specifically required for bubonic plague // Proc. Natl. Acad. Sci. USA. — 2006. — V. 103, N 36. — P. 13514–13519.
36. *Iriarte M., Vanooteghem J., Delor I. et al.* The Myf fibrillae of *Yersinia enterocolitica* // Mol. Microbiol. — 1993. — V. 9, N 3. — P. 507–520.
37. *Iriarte M., Cornelis G.* MyfF, an element of the network regulating the synthesis of fibrillae in *Yersinia enterocolitica* // J. Bacteriol. — 1995. — V. 177, N 3. — P. 738–744.
38. *Jalajakumar M., Thomas C., Halter R., Manning P.* Genes for biosynthesis and assembly of CS3 pili of CFA/II enterotoxigenic *Escherichia coli:* novel regulation of pilus production by bypassing an amber codon // Mol. Microbiol. — 1989. — V. 12, N 12. — P. 1685–1695.
39. *Ahrens R., Ott M., Ritter A. et al.* Genetic analysis of the gene cluster encoding nonfimbrial adhesin I from an *Escherichia coli* uropathogen // Infect. Immun. — 1993. — V. 61, N 6. — P. 2505–2512.
40. *Jouve M., Garcia M., Courcoux P. et al.* Adhesion to and invasion of HeLa cells by pathogenic *Escherichia coli* carrying the *afa-3* gene cluster are mediated by the AfaE and AfaD proteins, respectively // Ibid. — 1997. — V. 56, N 10. — P. 4082–4089.
41. *Servin A.* Pathogenesis of Afa/Dr diffusely adhering *Escherichia coli* // Clin. Microbiol. Rev. — 2005. — V. 18, N 2. — P. 264–292.
42. *Anderson K., Billington J., Pettigrew D. et al.* An atomic resolution model for assembly, architecture, and function of the Dr adhesions // Mol. Cell. — 2004. — V. 101, N 4. — P. 647–657.
43. *Anderson K., Cota E., Simpson P. et al.* Complete resonance assignments of a 'donor-strand complemented' AfaE: the afimbrial adhesin from diffusely adherent *E. coli* // J. Biomol. NMR. — 2004. — V. 29, N 3. — P. 409–410.
44. *Pettigrew D., Anderson K., Billington J. et al.* High resolution studies of the Afa/Dr adhesin DraE and its interaction with chloramphenicol // J. Biol. Chem. — 2004. — V. 279, N 45. — P. 46851–46857.
45. *Zalewska B., Pi tek R., Bury K. et al.* A surface-exposed DraD protein of uropathogenic *Escherichia coli* bearing Dr fimbriae may be expressed and secreted independently from DraC usher and DraE adhesion // Microbiology. — 2005. — V. 151, N 7. — P. 2477–2486.
46. *Zalewska-Piatek B., Bury K., Piatek R. et al.* Type II secretory pathway for surface secretion of DraD invasion from the uropathogenic *Escherichia coli* Dr1 strain // J. Bacteriol. — 2008. — V. 190, N 14. — P. 5044–5056.
47. *Korotkova N., Yarova-Yarovaya Y., Tchesnokova V. et al. Escherichia coli* DraE adhesin-associated bacterial internalization by epithelial cells is promoted independently by decay-accelerating factor and carcinoembryonic antigen-related cell adhesion molecule binding and does not require the DraD invasion // Infect. Immun. — 2008. — V. 76, N 9. — P. 3869–3880.
48. *Guignot J., Hudault S., Kansau I. et al.* DAF and CEACAMs receptor-mediated internalization and intracellular lifestyle of Afa/Dr diffusely adhering *Escherichia coli* into epithelial cells // Ibid. — 2009. — V. 77, N 1. — P. 517–531.
49. *Clouthier S., Collinson S., Kay W.* Unique fimbriae-like structures encoded by *sefD* of the SEF14 fimbrial gene cluster of *Salmonella enteritidis* // Mol. Microbiol. — 1994. — V. 12, N 6. — P. 893–901.
50. *Wolf M., De Haan L., Cassels F. et al.* The CS6 colonization factor of human enterotoxigenic *Escherichia coli* contains two heterologous major subunits // FEMS Microbiol. Lett. — 1997. — V. 148, N 1. — P. 35–42.
51. *Chessa D., Dorsey C., Winter M., Bäumler A.* Binding specificity of *Salmonella* plasmid-encoded fimbriae assessed by glycomics // J. Biol. Chem. — 2008. — V. 283, N 13. — P. 8118–8124.
52. *Bakker D., Vader C., Roosendaal B. et al.* Structure and function of periplasmic chaperone-like proteins involved in the biosynthesis of K88 and K99 fimbriae in enterotoxigenic *Escherichia coli* // Mol. Microbiol. — 1991. — V. 5, N 4. — P. 875–886.
53. *Adams L., Simmons C., Rezmann L. et al.* Identification and characterization of a K88- and CS31A-like operon of a rabbit enteropathogenic and K99 fimbriae in enterotoxigenic *Escherichia coli* // Ibid. — 1997. — V. 65, N 12. — P. 875–886.
54. *Scaletsky I., Michalski J., Torres A. et al.* Identification and characterization of the locus for diffuse adherence, which encodes a novel afimbrial adhesion found in atypical enteropathogenic *Escherichia coli* // Infect. Immun. — 2005. — V. 73, N 8. — P. 4753–4765.
55. *Van Molle I., Moonens K., Garcia-Pino A. et al.* Structural and thermodynamic characterization of pre- and postpolymerization states in the F4 fimbrial subunit FaeG // J. Mol. Biol. — 2009. — V. 394, N 5. — P. 957–967.
56. *Cantey J., Blake R., Williford J., Moseley S.* Characterization of the *Escherichia coli*

AF/R1 pilus operon: novel genes necessary for transcriptional regulation and for pilus-mediated adherence // Infect. Immun. — 1999. — V. 67, N 5. — P. 2292–2298.
57. *Imberechts H., Wild P., Charlier G. et al.* Characterization of F18 fimbrial genes *fedE* and *fedF* involved in adhesion and length of enterotoxemic *Escherichia coli* strain 107/86 // Microb. Pathog. — 1996. — V. 21, N 3. — P. 183–192.
58. *Smeds A., Hemmann K., Jakava-Viljanen M. et al.* Characterization of the adhesin of *Escherichia coli* F18 fimbriae // Infect. Immun. — 2001. — V. 69, N 12. — P. 7941–7945.
59. *Moonens K., Bouckaert J., Coddens A. et al.* Structural insight in histo-blood group binding by the F18 fimbrial adhesin FedF // Mol. Microbiol. — 2012. — V. 86, N 1. — P. 82–95.
60. *Martínez-Santos V., Medrano-López A., Saldaña Z. et al.* Transcriptional regulation of the *ecp* operon by EcpR, IHF, and H-NS in attaching and effacing *Escherichia coli* // J. Bacteriol. — 2012. — V. 194, N 18. — P. 5020–5033.
61. *Bann J., Pinkner J., Frieden C., Hultgren S.* Catalysis of protein folding by chaperones in pathogenic bacteria // Proc. Natl. Acad. Sci. USA. — 2004. — V. 101, N 50. — P. 17389–17393.
62. *Nishiyama M., Vetsch M., Puorger C. et al.* Identification and characterization of the chaperone subunit complex-binding domain from the Type 1 pilus assembly platform FimD // J. Mol. Biol. — 2003. — V. 330, N 3. — P. 513–525.
63. *Choudhury D., Thompson A., Stojanoff V. et al.* X-ray structure of the FimC-FimH chaperone–adhesin complex from uropathogenic *Escherichia coli* // Science. — 1999. — V. 285, N 5430. — P. 1061–1066.
64. *Sauer F., Futterer K., Pinkner J. et al.* Structural basis of chaperone function and pilus biogenesis // Science. — 1999. — V. 285, N 5430. — P. 1058–1061.
65. *Sauer F., Pinkner J., Waksman G., Hultgren S.* Chaperone priming of pilus subunits facilitates a topological transition that drives fiber formation // Cell. — 2002. — V. 111, N 4. — P. 543–551.
66. *Remaut H., Rose R., Hannan T. et al.* Donor-strand exchange in chaperone-assisted pilus assembly proceeds through a concerted β strand displacement mechanism // Mol. Cell. — 2006. — V. 22, N 6. — P. 831–842.
67. *Verger D., Bullitt E., Hultgren S., Waksman G.* Crystal structure of the P pilus rod subunit PapA // PLoS Pathogens. — 2007. — V. 3. — P. e73.
68. *Bork P., Holm L., Sander C.* The immunoglobulin fold: structural classification, sequence patterns and common core // J. Mol. Biol. — 1994. — V. 242, N 4. — P. 309–320.
69. *DeLano W.* Unraveling hot spots in binding interfaces: progress and challenges // Curr. Opin. Struct. Biol. — 2002. — V. 12, N 1. — P. 14–20.
70. *Jacob-Dubuisson F., Striker R., Hultgren S.* Chaperone assisted self-assembly of pili independent of cellular energy // J. Biol. Chem. — 1994. — V. 269, N 17. — P. 12447–12455.
71. *Fronzes R., Remaut H., Waksman G.* Architectures and biogenesis of non-flagellar protein appendages in Gram-negative bacteria // EMBO J. — 2008. — V. 27, N 17. — P. 2271–2280.
72. *Thanassi D., Saulino E., Hultgren S.* The chaperone/usher pathway: a major terminal branch of the general secretory pathway // Curr. Opin. Microbiol. — 1998. — V. 1, N 2. — P. 223–231.
73. *Soto G., Hultgren S.* Bacterial adhesins: common themes and variations in architecture and assembly // J. Bacteriol. — 1999. — V. 181. N 4. — P. 1059–1071.
74. *Knight S., Berglund J., Choudhury D.* Bacterial adhesins: structural studies reveal chaperone function and pilus biogenesis // Curr. Opin. Chem. Biol. — 2000. — V. 4, N 6. — P. 653–660.
75. *Sauer F., Barnhart M., Choudhury D. et al.* Chaperone-assisted pilus assembly and bacterial attachment // Ibid. — 2000. — V. 10, N 5. — P. 548–556.
76. *Sauer F., Remaut H., Hultgren S., Waksman G.* Fiber assembly by the chaperone–usher pathway // Biochim. Biophys. Acta. — 2004. — V. 1694, N 1–3. — P. 259–267.
77. *Van den Broeck W., Cox E., Oudega C., Goddeeris B.* The F4 fimbrial antigen of *Escherichia coli* and its receptors // Vet. Microbiol. — 2000. — V. 71, N 3–4. — P. 223–244.
78. *Roy S., Rahman M., Yu X. et al.* Crystal structure of enterotoxigenic *Escherichia coli* colonization factor CS6 reveals a novel type of functional assembly // Mol. Microbiol. — 2012. — V. 86, N 5. — P. 1100–1115.
79. *Chen T., Elberg S.* Scanning electron microscopic study of virulent *Yersinia pestis* and *Yersinia pseudotuberculosis* type 1 // Infect. Immun. — 1977. — V. 15, N 3. — P. 972–977.
80. *Pham T., Goluszko P., Popov V. et al.* Molecular cloning and characterization of Dr-II A nonfimbrial adhesin-I-like adhesin isolated from gestational pyelonephritis-associated Escherichia coli that binds to decayaccelerating factor // Ibid. — 1997. — V. 65, N 10. — P. 4309–4318.
81. *Lalioui L., Jouve M., Gounon P., Le Bouguénec C.* Molecular cloning and characterization of the *afa-7* and *afa-8* gene clusters encoding afimbrial adhesins in *Escherichia coli* strains associated with diarrhea or septicemia in calves // Ibid. — 1999. — V. 67, N 10. — P. 5048–5059.
82. *De Greve H., Wyns L., Bouckaert J.* Combining sites of bacterial fimbriae // Curr. Opin. Struct. Biol. — 2007. — V. 17, N 5. — P. 506–512.
83. *Westerlund-Wikström B., Korhonen T.* Molecular structure of adhesin domains in *Escherichia coli* fimbriae // Int. J. Med. Microbiol. — 2005. — V. 295, N 6–7. — P. 479–486.

84. *Bouckaert J., Berglund J., Schembri M. et al.* Receptor binding studies disclose a novel class of high-affinity inhibitors of the *Escherichia coli* FimH adhesion // Mol. Microbiol. — 2005. — V. 55, N 2. — P. 441–455.
85. *Bouckaert J., Mackenzie J., de Paz J. et al.* The affinity of the FimH fimbrial adhesin is receptor-driven and quasiindependent of *Escherichia coli* pathotypes // Ibid. — 2006. — V. 61, N 6. — P. 1556–1568.
86. *Li Y., Poole S., Rasulova F. et al.* A receptor-binding site as revealed by the crystal structure of CfaE, the colonization factor antigen I fimbrial adhesin of enterotoxigenic *Escherichia coli* // J. Biol. Chem. — 2006. — V. 282, N 33. — P. 23970–23980.
87. *Lindberg F., Lund B., Johansson L., Normark S.* Localization of the receptor binding protein adhesin at the tip of the bacterial pilus // Nature. — 1987. — V. 328, N 6125. — P. 84–87.
88. *Kuehn M., Heuser J., Normark S., Hultgren S.* P pili in uropathogenic *E. coli* are composite fibres with distinct fibrillar adhesive tips // Ibid. — 1992. — V. 356, N 6366. — P. 252–255.
89. *Korotkova N., Cota E., Lebedin Y. et al.* A subfamily of Dr adhesions of *Escherichia coli* bind independently to decay-accelerating factor and the N-domain of carcinoembrionic antigen // J. Biol. Chem. — 2006. — V. 281, N 39. — P. 29120–29130.
90. *Korotkova N., Le Trong I., Samudrala R. et al.* Crystal structure and mutational analysis of the DaaE adhesin of *Escherichia coli* // Ibid. — 2006. — V. 281, N 31. — P. 22367–22377.
91. *Korotkova N., Yang Y., Le Trong I. et al.* Binding of Dr adhesins of *Escherichia coli* to carcinoembryonic antigen triggers receptor dissociation // Mol. Microbiol. — 2008. — V. 67, N 2. — P. 420–434.
92. *Runco L., Myrczek S., Bliska J., Thanassi D.* Biogenesis of the fraction 1 capsule and analysis of the ultrastructure of *Yersinia pestis* // J. Bacteriol. — 2008. — V. 190, N 9. — P. 3381–3385.
93. *Du Y., Rosqvist R., Forsberg E.* Role of fraction 1 antigen of *Yersinia pestis* in inhibition of phagocytosis // Infect. Immun. — 2002. — V. 70, N 3. — P. 1453–1460.
94. *Liu F., Chen H., Galván E. et al.* Effects of Psa and F1 on the adhesive and invasive interactions of *Yersinia pestis* with human respiratory tract epithelial cells // Ibid. — 2006. — V. 74, N 10. — P. 5636–5644.
95. *Levine M., Ristaino P., Marley G. et al.* Coli surface antigens 1 and 3 of colonization factor antigen II-positive enterotoxigenic *Escherichia coli*: morphology, purification, and immune responses in humans // Ibid. — 1984. — V. 44, N 2. — P. 409–420.
96. *Knutton S., McConnel M., Rowe B., McNeish A.* Adhesion and ultrastructural properties of human enterotoxigenic *Escherichia coli* producing colonization factor antigens III and IV // Ibid. — 1989. — V. 57, N 11. — P. 3364–3371.
97. *Salih O., Remaut H., Waksman G., Orlova E.* Structural analysis of the Saf pilus by electron microscopy and image processing // J. Mol. Biol. — 2008. — V. 379, N 1. — P. 174–187.
98. *Cornelis G., Wolf-Watz H.* The *Yersinia* Yop virulon: a bacterial system for subverting eukaryotic cells // Mol. Microbiol. — 1997. — V. 23, N 5. — P. 861–867.
99. *Viboud G., Bliska J. Yersinia* outer proteins: role in modulation of host cell signaling responses and pathogenesis // Annu. Rev. Microbiol. — 2005. — V. 59. — P. 69–89.
100. *Cornelis G.* The type III secretion injectisome, a complex nanomachine for intracellular 'toxin' delivery // J. Biol. Chem. — 2010. — V. 391, N 7. — P. 745–751.
101. *Diepold A., Amstutz M., Abel S. et al.* Deciphering the assembly of the *Yersinia* type III secretion injectisome // EMBO J. — 2010. — V. 29, N 11. — P. 1928–1940.
102. *Marketon M., Depaolo R., Debord K. et al.* Plague bacteria target immune cells during infection // Science. — 2005. — V. 309, N 5741. — P. 1739–1741.
103. *Velan B., Bar-Haim E., Zauberman A. et al.* Discordance in the effects of *Yersinia pestis* on dendritic cell functions: induction of maturation and paralysis of migration // Infect. Immun. — 2006. — V. 74, N 11. — P. 6365–6376.
104. *Felek S., Tsang T., Krukonis E.* Three *Yersinia pestis* adhesins facilitate Yop delivery to eukaryotic cells and contribute to plague virulence // Ibid. — 2010. — V. 78, N 10. — P. 4134–4150.
105. *Nowicki B., Moulds J., Hull R., Hull S.* A hemagglutinin of uropathogenic *Escherichia coli* recognizes the Dr blood group antigen // Ibid. — 1988. — V. 56, N 5. — P. 1057–1060.
106. *Fujita T., Inoue T., Ogawa K. et al.* The mechanism of action of decay-accelerating factor (DAF) DAF inhibits the assembly of C3 convertases by dissociating C2a and Bb // J. Exp. Med. — 1987. — V. 166, N 5. — P. 1221–1228.
107. *Lublin D., Atkinson J.* Decay-accelerating factor: biochemistry, molecular biology, and function // Annu. Rev. Immunol. — 1989. — V. 7. P. 35–58.
108. *Westerlund B., Kuusela P., Risteli J. et al.* The O75X adhesin of uropathogenic *Escherichia coli* is a type IV collagen-binding protein // Mol. Microbiol. — 1989. — V. 3, N 3. — P. 329–337.
109. *Berger C., Billker O., Meyer T. et al.* Differential recognition of members of the carcinoembryonic antigen family by Afa/Dr adhesins of diffusely adhering *Escherichia coli* (Afa/Dr DAEC) // Ibid. — 2004. — V. 52, N 4. — P. 963–983.

110. *Öbrink B.* CEA adhesion molecules: multifunctional proteins with signal-regulatory properties // Curr. Opin. Cell. Biol. — 1997. — V. 9, N 5. — P. 616–626.
111. *Grunert F., Kuroki M.* CEA family members expressed on hematopoeitic cells and their possible role in cell adhesion and signaling // Cell Adhesion and Communication Mediated by the CEA Family-Basic and Clinical Perspective (Stanners CP, ed) Harwood Academic Publishers, Amsterdam, 1999. — P. 99–120.
112. *Benchimol S., Fuks A., Jothy S. et al.* Carcinoembryonic antigen, a human tumor marker, functions as an intercellular adhesion molecule // Cell. — 1989. — V. 57, N 2. — P. 327–334.
113. *Kammerer R., Hahn S., Singer B. et al.* Biliary glycoprotein (CD66a), a cell adhesion molecule of the immunoglobulin superfamily, on human lymphocytes: structure, expression and involvement in T cell activation // Eur. J. Immunol. — 1998. — V. 28, N 11. — P. 3664–3674.
114. *Kammerer R., Stober D., Singer B. et al.* Carcinoembryonic antigen-related cell adhesion molecule 1 on murine dendritic cells is a potent regulator of T cell stimulation // J. Immunol. — 2001. — V. 166, N 11. — P. 6537–6544.
115. *Nakajima A., Iijima H., Neurath M. et al.* Activation-induced expression of carcinoembryonic antigen-cell adhesion molecule 1 regulates mouse T lymphocyte function // Ibid. — 2002. — V. 168, N 3. — P. 1028–1035.
116. *Fahlgren A., Baranov V., Frangsmyr L. et al.* Interferon-gamma tempers the expression of carcinoembryonic antigen family molecules in human colon cells: a possible role in innate mucosal defence // Scand. J. Immunol. — 2003. — V. 58, N 6. — P. 628–641.
117. *Van Molle I., Joensuu J., Buts L. et al.* Chloroplasts assemble the major subunit FaeG of *Escherichia coli* F4 (K88) fimbriae to strand-swapped dimmers // J. Mol. Biol. — 2007. — V. 368, N 3. — P. 791–799.
118. *Zav'yalov V., Abramov V., Cherepanov P. et al.* pH6 antigen (PsaA protein) of *Yersinia pestis*, a novel bacterial Fc-receptor // FEMS Immunol. Med. Microbiol. — 1996. — V. 14, N 1. — P. 53–57.
119. *Payne D., Tatham D., Williamson E., Titball R.* pH6 antigen of *Yersinia pestis* binds to β1-linked galactosyl residues in glycosphingolipids // Infect. Immun. — 1998. — V. 66, N 9. — P. 4545–4548.
120. *Deisenhofer J.* Crystallographic refinement and atomic models of a human Fc fragment and its complex with fragment B of protein A from *Staphylococcus aureus* at 2.9- and 2.8-E resolution // Biochemistry. — 1981. — V. 20, N 9. — P. 2361–2370.
121. *Makoveichuk E., Cherepanov P., Lundberg S. et al.* pH6 antigen of *Yersinia pestis* interacts with plasma lipoproteins and cell membranes // Lipid Res. — 2003. — V. 44, N 2. — P. 320–330.
122. *Galván E., Chen H., Schifferli D.* The Psa fimbriae of *Yersinia pestis* interact with phosphatidylcholine on alveolar epithelial cells and pulmonary surfactant // Infect. Immun. — 2006. — V. 75, N 3. — P. 1272–1279.
123. *Bao R., Nair M., Tang W. et al.* Structural basis for the specific recognition of dual receptors by the homopolymeric pH 6 antigen (Psa) fimbriae of *Yersinia pestis* // Proc. Natl. Acad. Sci. USA. — 2013. — V. 110, N 3. — P. 1065–1070.
124. *Pouttu R., Westerlund-Wikstrom B., Lang H. et al.* Matb, a common fimbrillin gene of *Escherichia coli*, expressed in a genetically conserved, virulent clonal group // J. Bacteriol. — 2001. — V. 183, N 16. — P. 4727–4736.
125. *Rendon M., Saldana Z., Erdem A. et al.* Commensal and pathogenic *Escherichia coli* use a common pilus adherence factor for epithelial cell colonization // Proc. Natl. Acad. Sci. USA. — 2007. — V. 104, N 25. — P. 10637–10642.
126. *Saldana Z., Erdem A., Schuller S. et al.* The *Escherichia coli* common pilus and the bundle-forming pilus act in concert during the formation of localized adherence by enteropathogenic *E. coli* // J. Bacteriol. — 2009. — V. 191, N 11. — P. 3451–3461.
127. *Blackburn D., Husband A., Saldana Z. et al.* Distribution of the *Escherichia coli* common pilus among diverse strains of human enterotoxigenic *E. coli* // J. Clin. Microbiol. — 2009. — V. 47, N 6. — P. 1781–1784.
128. *Avelino F., Saldana Z., Islam S. et al.* The majority of enteroaggregative *Escherichia coli* strains produce the *E. coli* common pilus when adhering to cultured epithelial cells // Int. J. Med. Microbiol. — 2010. — V. 300, N 7. — P. 440–448.
129. *Croxen M., Finlay B.* Molecular mechanisms of *Escherichia coli* pathogenicity // Nat. Rev. Microbiol. — 2010. — V. 8, N 1. — P. 26–38.
130. *Picard B., Garcia J., Gouriou S. et al.* The link between phylogeny and virulence in *Escherichia coli* extraintestinal infection // Infect. Immun. — 1999. — V. 67, N 2. — P. 546–553.
131. *Lehti T., Bauchart P., Heikkinen J. et al.* Mat fimbriae promote biofilm formation by meningitis-associated *Escherichia coli* // Microbiology. — 2010. — V. 156, N 8. — P. 2408–2417.
132. *Zhang W., Sack D.* Progress and hurdles in the development of vaccines against enterotoxigenic *Escherichia coli* in humans // Expert Rev. Vaccines. — 2012. — V. 11, N 6. — P. 677–694.
133. *De Jong B., Ekdahl B.* The comparative burden of salmonellosis in the European Union member states, associated and candidate countries // BMC Public Health. — 2006. — V. 6. — P. 4.

134. *Giske C., Monnet D., Cars O., Carmeli Y.* Clinical and economic impact of common multidrug-resistant Gram-negative bacilli // Antimicrob. Agents Chemother. — 2008. — V.52, N 3. — P. 813–821.

135. *Rasko D., Webster D., Sahl J. et al.* Origins of the *E. coli* strain causing an outbreak of hemolytic–uremic syndrome in Germany // N. Engl. J. Med. — 2011. — V. 365, N 8. — P. 709–717.

ПОЛІАДГЕЗИНИ: ЗАСІБ ДЛЯ ПРОНИКНЕННЯ ГРАМНЕГАТИВНИХ ПАТОГЕНІВ КРІЗЬ ІМУННИЙ БАР'ЄР

В. П. Зав'ялов[1, 2]

[1]Спільна лабораторія біотехнології, хімічний факультет, Університет Турку, Турку, Фінляндія
[2]Херсонський державний університет, Херсон, Україна

E-mail: vlazav@utu. fi

Швидка поява резистентних до лікування бактеріальних патогенів стала однією з основних небезпек для здоров'я населення. Нещодавній спалах інфекції нового шига-токсину кишкової палички O104H4 в Німеччині ілюструє цю проблему. Для колонізації тканин хазяїна патогенні бактерії експресують поверхнево-адгезивні органели. Німецький штам використовує агрегативний імунний адгезив *fimbriae I* для прикріплення до слизової оболонки кишечника, спричинюючи запалення. *Fimbriae I* належить до родини шаперонпровідних асоційованих фімбріальних поліадгезинів, що функціонують як механізм проникнення крізь імунний бар'єр хазяїна. Зв'язування поліадгезинів із клітинами-мішенями координується інфектисомою (третя система секреції), що вкрай важливо для вияву бактеріальної вірулентності і сприяє індукції деструктивних сигналів агрегації рецепторів клітини-хазяїна, які дають змогу патогенам ввести в клітину хибну інформацію та проникнути через імунний бар'єр. Поліадгезини також залучені в утворення біоплівки, що робить бактерії стійкішими до імунної відповіді. З огляду на це поліадгезини є потенційними мішенями для розроблення контрметодів імунного захисту проти бактерійних інфекцій, зокрема антиадгезивної терапії відповідними антитілами як однієї з альтернатив антибіотикотерапії.

Ключові слова: грамнегативні патогени, поліадгезини, подолання імунного бар'єра.

ПОЛИАДГЕЗИНЫ: СРЕДСТВО ДЛЯ ПРОНИКНОВЕНИЯ ГРАММОТРИЦАТЕЛЬНЫХ ПАТОГЕНОВ ЧЕРЕЗ ИММУННЫЙ БАРЬЕР

В. П. Завьялов[1, 2]

[1]Совместная лаборатория биотехнологии, химический факультет, Университет Турку, Турку, Финляндия
[2]Херсонский государственный университет, Херсон, Украина

E-mail: vlazav@utu. fi

Быстрое появление резистентных к лечению бактериальных патогенов стало одной из основных опасностей для здоровья населения. Недавняя вспышка инфекции нового шига-токсина кишечной палочки O104H4 в Германии иллюстрирует эту проблему. Для колонизации тканей хозяина патогенные бактерии экспрессируют поверхностно-адгезивные органеллы. Немецкий штамм использует агрегативный иммунный адгезив *fimbriae I* для прикрепления к слизистой оболочке кишечника, вызывая воспаление. *Fimbriae I* принадлежит к семейству шаперонпроводящих ассоциированных фимбриальных полиадгезинов, которые функционируют в качестве механизма проникновения через иммунный барьер хозяина. Связывание полиадгезинов с клетками-мишенями координируется инфектисомой (третья система секреции), что крайне важно для проявления бактериальной вирулентности и способствует индукции деструктивных сигналов агрегации рецепторов клетки-хозяина, позволяющих патогенам ввести в клетку ложную информацию и проникнуть через иммунный барьер. Полиадгезины также вовлечены в образование биопленки, которая делает бактерии более устойчивыми к иммунному ответу. Поэтому полиадгезины являются потенциальными мишенями для разработки контрметодов иммунной защиты против бактерийных инфекций, в частности антиадгезивной терапии соответствующими антителами как одной из альтернатив антибиотикотерапии.

Ключевые слова: граммотрицательные патогены, полиадгезины, преодоление иммунного барьера.